Whole-exome sequencing-based discovery of STIM1 deficiency in a child with fatal classic Kaposi sarcoma

Minji Byun,[1] Avinash Abhyankar,[1] Virginie Lelarge,[2] Sabine Plancoulaine,[3,4] Ayse Palanduz,[5] Leyla Telhan,[6] Bertrand Boisson,[1] Capucine Picard,[3,4,7] Scott Dewell,[8] Connie Zhao,[8] Emmanuelle Jouanguy,[1,3,4] Stefan Feske,[2] Laurent Abel,[1,3,4] and Jean-Laurent Casanova[1,3,4,9]

[1]St. Giles Laboratory of Human Genetics of Infectious Diseases, Rockefeller Branch, The Rockefeller University, New York, NY 10065
[2]Department of Pathology, New York University, Langone Medical Center, New York, NY 10016
[3]Laboratory of Human Genetics of Infectious Diseases, Necker Branch, Institut National de la Santé et de la Recherche Médicale, U980, 75015 Paris, France
[4]Paris Descartes University, Necker Medical School, 75015 Paris, France
[5]Department of Family Medicine, Istanbul Faculty of Medicine, Istanbul University, Istanbul, Turkey
[6]Department of Pediatric Infectious Diseases, Sisli Etfal Training and Research Hospital, Istanbul, Turkey
[7]Study Center of Immunodeficiencies, Necker Hospital, AP-HP, 75015 Paris, France
[8]Genomics Resource Center, The Rockefeller University, New York, NY 10065
[9]Pediatric Hematology-Immunology Unit, Necker Hospital, AP-HP, 75015 Paris, France

Classic Kaposi sarcoma (KS) is exceedingly rare in children from the Mediterranean Basin, despite the high prevalence of human herpesvirus-8 (HHV-8) infection in this region. We hypothesized that rare single-gene inborn errors of immunity to HHV-8 may underlie classic KS in childhood. We investigated a child with no other unusually severe infectious or tumoral phenotype who died from disseminated KS at two years of age. Whole-exome sequencing in the patient revealed a homozygous splice-site mutation in *STIM1*, the gene encoding stromal interaction molecule 1, which regulates store-operated Ca^{2+} entry. *STIM1* mRNA splicing, protein production, and Ca^{2+} influx were completely abolished in EBV-transformed B cell lines from the patient, but were rescued by the expression of wild-type STIM1. Based on the previous discovery of STIM1 deficiency in a single family with a severe T cell immunodeficiency and the much higher risk of KS in individuals with acquired T cell deficiencies, we conclude that STIM1 T cell deficiency precipitated the development of lethal KS in this child upon infection with HHV-8. Our report provides the first evidence that isolated classic KS in childhood may result from single-gene defects and provides proof-of-principle that whole-exome sequencing in single patients can decipher the genetic basis of rare inborn errors.

CORRESPONDENCE
Jean-Laurent Casanova:
jean-laurent.casanova@rockefeller.edu
OR
Minji Byun:
miby769@rockefeller.edu

Abbreviations used: HHV-8, human herpesvirus-8; KS, Kaposi sarcoma; STIM1, stromal interaction molecule 1; SOCE, store-operated calcium entry.

Kaposi sarcoma (KS) is an angiogenic, inflammatory neoplasm first described by Moritz Kaposi (1872). The etiology of KS was unknown until Chang et al. (1994) isolated KS-associated herpesvirus, also known as human herpesvirus (HHV)-8, from KS lesions. Cells of endothelial origin are the principal targets of HHV-8 infection and the major components proliferating in KS lesions (Ganem, 2010). It has been clearly established that all forms of KS are associated with HHV-8 (Dupin et al., 1995; Moore and Chang, 1995; Schalling et al., 1995; Chang et al., 1996). Infection with HHV-8 is necessary but not sufficient for the development of KS. Despite the high seroprevalence of HHV-8, at up to 30% in the Mediterranean Basin (classic KS) and 70% in sub-Saharan Africa (endemic KS), the incidence of KS is very low (Boshoff and Weiss, 2001). Individuals with acquired immunodeficiency caused by HIV

A. Abhyankar, V. Lelarge, and S. Plancoulaine contributed equally to this paper.

The Rockefeller University Press $30.00
J. Exp. Med. Vol. 207 No. 11 2307-2312
www.jem.org/cgi/doi/10.1084/jem.20101597

The Journal of Experimental Medicine

infection (epidemic KS; Martellotta et al., 2009) or immunosuppression after organ transplantation (iatrogenic KS; Lebbé et al., 2008) are at a much higher risk of developing KS than the general population. Host factors in other patients are therefore likely to play a critical role in determining the outcome of HHV-8 infection, including the development of KS in particular.

As a first approach to testing the hypothesis that KS may result from inborn errors of immunity to HHV-8 in some patients (Casanova and Abel, 2007), we focused on classic KS in childhood. Classic KS is exceedingly rare in children, with only 30 cases reported since 1960, and follows a disseminated and often lethal course (Dutz and Stout, 1960; Bisceglia et al., 1988; Akman et al., 1989; Zurrida et al., 1994; Erdem et al., 1999; Landau et al., 2001; Ferrari et al., 2002; Hussein, 2008). We previously reported two children from the Mediterranean Basin with KS caused by an underlying primary immunodeficiency, one with autosomal recessive complete IFN-γR-1 deficiency (Camcioglu et al., 2004) and the other with X-linked recessive Wiskott-Aldrich syndrome (Picard et al., 2006). These children had several other clinical phenotypes, including mycobacterial disease in the IFN-γR1–deficient child and EBV-driven lymphoma in the child with Wiskott-Aldrich syndrome. These two cases provided the first evidence that classic KS in childhood may result from inborn errors of immunity, at least in children with multiple infectious and tumoral phenotypes, including KS.

More recently, we described three unrelated Turkish children with classic KS in the absence of any other infectious or tumoral phenotype, each born to consanguineous parents (Sahin et al., 2010). This suggested that classic KS in children with no overt signs of immunodeficiency might also result from single-gene defects impairing HHV-8 immunity. Because the age of onset, clinical features, and outcome of KS reported in previous studies differ from child to child (Dutz and Stout, 1960; Bisceglia et al., 1988; Akman et al., 1989; Zurrida et al., 1994; Erdem et al., 1999; Landau et al., 2001; Ferrari et al., 2002; Picard et al., 2006; Camcioglu et al., 2004; Hussein, 2008; Sahin et al., 2010), we further hypothesized that the single-gene inborn errors of immunity underlying classic KS in children are heterogeneous. We focused our investigation on a single Turkish child with early-onset disseminated KS that eventually ran a lethal course, using the recently developed whole-exome sequencing approach, which has been used to determine the genetic basis of other rare Mendelian disorders in small numbers of affected individuals (Choi et al., 2009; Hoischen et al., 2010; Lalonde et al., 2010; Ng et al., 2010; Walsh et al., 2010).

RESULTS AND DISCUSSION

The patient was born to consanguineous parents of Turkish origin. A detailed case report has been published elsewhere (case 1; Sahin et al., 2010). In brief, at 2 yr of age, the patient developed a first KS lesion on the lip, which was followed by rapid dissemination throughout the body. She had lymphadenopathy and hepatosplenomegaly, and she died from severe pulmonary lesions 4 mo later. She had no history of other severe infections or tumors, but presented autoimmune hemolytic anemia. The counts and proportions of blood T, B, and NK cells and subsets were normal, as were serum immunoglobulin levels. T cell responses to mitogens and antigens were not tested. Serologic tests for HIV were negative, and KS was diagnosed on the basis of skin biopsies demonstrating the presence of spindle cells and positive staining for HHV-8 in situ. Our investigations of the genetic basis of KS in this child did not begin until after she had died.

We hypothesized that this child might have carried a homozygous mutation in a gene important for immunity to HHV-8, given the consanguinity of her parents. We searched for candidate mutations by massive parallel sequencing of the patient's exome (Table I). Identified substitutions and insertions/deletions (indels) were screened with the following criteria: (a) not found in dbSNP 129, 1000 genomes, or in-house database (composed of 49 exomes); (b) predicted to have one of the following functional impacts: nonsense, missense, splice-site mutations, or coding indels; (c) homozygous. 1 splice-site mutation and 11 missense mutations fulfilled all these criteria. The splice-site mutation was at a consensus splice acceptor site in *STIM1*, which was retained as a strong candidate gene for predisposition to KS, based on the recent description of a family with autosomal recessive STIM1 deficiency and primary T cell immunodeficiency (Picard et al., 2009). In contrast, none of the 11 genes carrying missense mutations were clearly implicated in immunity or selectively expressed in endothelial cells (Table S1). We confirmed the variation in *STIM1*, a G to A substitution at the −1 position of 5′-exon 8 (1,538–1G>A), by Sanger sequencing (Fig. 1 A). This variation was not found in 100 healthy Turkish control subjects (total of 200 chromosomes), suggesting that it is not an irrelevant polymorphism and may be a rare allele conferring predisposition to KS. No additional unreported variation in

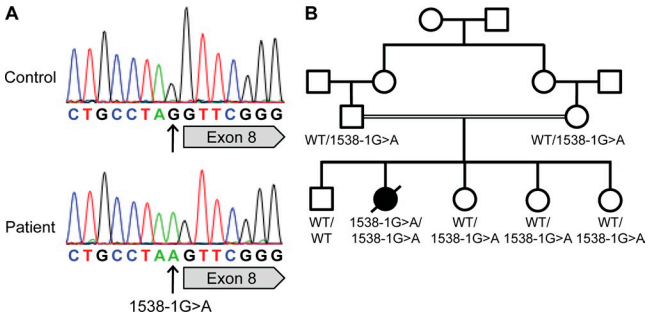

Figure 1. Identification of a splice-site mutation in *STIM1*. (A) Sanger sequencing of genomic DNA confirmed G to A substitution at the −1 position of *STIM1* exon 8 (1538-1G>A) in the patient, which was initially identified by whole-exome sequencing. Sequencing of genomic DNA extracted from EBV-B cells of a healthy control shows the reference base G at the same position. (B) *STIM1* genotypes of the patient and her family members from whom DNA was available for sequence analysis are listed under their symbols. Squares, males; circles, females; filled symbol, affected individual; open symbols, unaffected individuals; double horizontal line, consanguineous marriage. Genotyping was performed twice.

Table I. Summary statistics for exome sequencing

Reads/variants	No.
Total number of reads	30,054,578
Uniquely mapped reads	13,267,598
Total variants called	20,108
Substitutions	
Total (novel[a])	18,891 (1,416)
Synonymous (novel[a])	3,270 (169)
Nonsense (novel[a])	19 (4)
Missense (novel[a])	2,718 (414)
Splice-site (novel[a])	8 (4)
Indels	1,217
dbSNP rate[b]	92.50%
dbSNP concordance[b]	99.68%

[a]Number of variants not found in dbSNP129 and 1000 genomes.
[b]dbSNP rate and concordance are based on dbSNP129.

STIM1 coding sequences and essential splice sites (−1 and −2 positions) was found in the patient. The familial segregation of the mutant *STIM1* allele was consistent with an autosomal recessive trait (Fig. 1 B).

We investigated the impact of this mutation on the biosynthesis and function of the STIM1 protein by studying EBV-transformed B cells (EBV-B cells) from the patient. No other material was available from the deceased patient. Quantitative RT-PCR demonstrated that levels of *STIM1* mRNA were lower (30%) in the patient's cells than in healthy control cells (Fig. 2 A). We investigated a possible impairment of the splicing of exon 8 in the patient's cells, by amplifying cDNA fragments corresponding to exons 7–9 of *STIM1* from the EBV-B cells of healthy controls and the patient. The PCR products were cloned and sequenced. Wild-type transcripts were completely lacking from the patient's cells, which contained only abnormally spliced variants (Fig. 2 B). As expected, given the absence of wild-type transcripts, no wild-type STIM1 protein was detected in the patient's EBV-B cells, whereas high levels of wild-type STIM1 protein were found in cells from healthy individuals, as shown by Western blotting with two different STIM1-specific antibodies (Fig. 2 C). No other protein band corresponding to the translation products of abnormally spliced variants was detected in the patient's EBV-B cells (unpublished data).

The complete lack of protein production detected suggested that STIM1 function would also be severely impaired, if not completely abolished. STIM1, an ER-resident transmembrane protein, senses the depletion of ER Ca^{2+} stores and activates the calcium release–activated calcium channel consisting of ORAI1 in the plasma membrane (Feske, 2009). This process is referred to as store-operated Ca^{2+} entry (SOCE). Upon treatment with thapsigargin, an inhibitor of the sarco/endoplasmic reticulum Ca^{2+}-ATPase that induces Ca^{2+} depletion in the ER, a small increase in intracellular Ca^{2+} concentration corresponding to the release of Ca^{2+} from ER stores in the absence of extracellular Ca^{2+} was observed in healthy control EBV-B cells (Fig. 3 A). This small increase was followed by a larger, sustained influx of Ca^{2+} upon readdition of extracellular Ca^{2+}. In contrast, the influx of extracellular Ca^{2+} was completely abolished in the patient's EBV-B cells, despite normal Ca^{2+} release from the ER stores (Fig. 3 A). The retrovirus-mediated production of wild-type STIM1 restored SOCE in the patient's cells, demonstrating that STIM1 deficiency was indeed the cause of impaired SOCE (Fig. 3 B). Thus, the child had complete STIM1 deficiency, caused by the inheritance of a homozygous loss-of-function STIM1 allele.

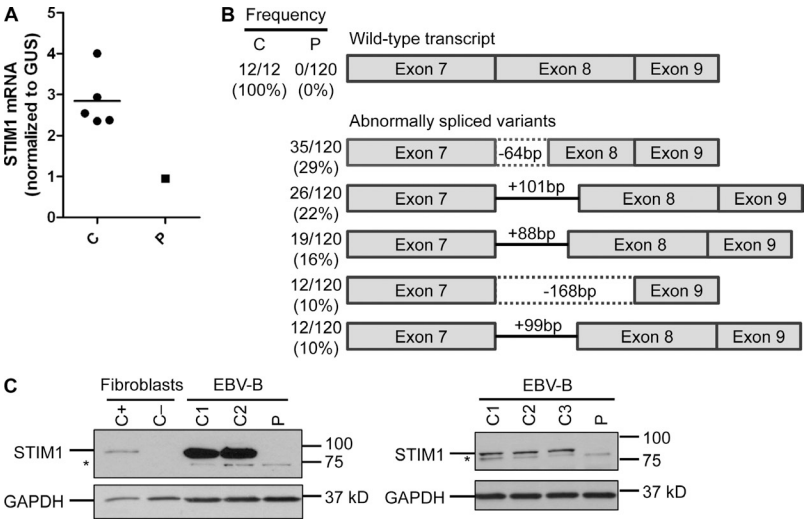

Figure 2. Abnormal STIM1 mRNA splicing and lack of protein expression in the patient's EBV-B cells. (A) Levels of STIM1 mRNA were assessed by quantitative RT-PCR in the EBV-B cells from five healthy controls (C) and the patient (P). Threshold cycles (C_T) for STIM1, normalized to those of GUS (ΔC_T), are plotted as $2^{-(\Delta CT)}$. Each dot or square represents a mean of three independent experiments for each individual. The horizontal bar indicates the mean of five healthy controls. (B) *STIM1* exons 7–9 were amplified from cDNA from EBV-B cells of the control (C) or the patient (P) and ligated to pCR2.1 vector. Clones containing *STIM1* transcripts were sequenced, and the frequency of each splice variant was calculated by dividing the number of clones containing the particular transcript by the total number of sequenced clones (n = 12 for C, n = 120 for P). 16/120 of P clones corresponded to other minor abnormal transcript forms (not depicted). Number of base pairs indicated between the exons in abnormally spliced variants of the patient represents the size of gain or loss, compared with the wild-type transcript. (C) Levels of STIM1 protein were assessed by immunoblotting with an antibody against the C terminus (left) or N terminus (right) of STIM1. Two fibroblast cell lines, derived from either a healthy individual (C+) or a previously reported STIM1-deficient patient (C−; Picard et al., 2009), were used as controls. C1, C2, and C3 show EBV-B cells from healthy controls and P shows EBV-B cells from the patients. GAPDH blots show comparable protein loading for each sample. Asterisks indicate nonspecific protein bands. Representative blots of three independent experiments are shown.

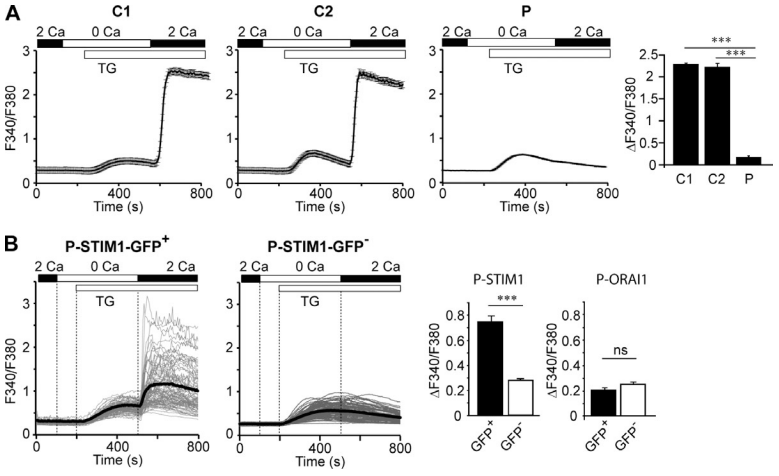

Figure 3. Abolished Ca^{2+} influx in the patient's EBV-B cells is restored by expression of STIM1. (A) EBV-B cells of the patient (P) and two controls (C1 and C2) were stimulated with 1 µM thapsigargin (TG) in Ca^{2+}-free Ringer solution (open bars) followed by perfusion with 2 mM Ca^{2+} (filled bars) to induce Ca^{2+} influx. Traces represent mean F340/F380 emission ratios of one representative experiment. Averages on the right are from $n = 6$ (C1), $n = 4$ (C2), $n = 5$ (P) experiments. ΔF340/F380 represents peak $[Ca^{2+}]_i$ 25 s after readdition of Ca^{2+} minus baseline $[Ca^{2+}]_i$ at the beginning of the recording. Error bars represent the SEM. ***, $P < 0.0001$. (B) EBV-B cells from the patient were retrovirally transduced with STIM1-IRES-GFP expression vector (P-STIM1) or ORAI1-IRES-GFP vector (P-ORAI1). Ca^{2+} levels were measured as described in A. Traces of individual cells (thin gray lines) and averages of all cells (thick black lines) are shown for 90 GFP^+ and 90 GFP^- cells. Averages of peak ΔF340/F380 from total 368 cells (P-STIM1; $n = 6$ experiments) or 482 cells (P-ORAI1; $n = 10$ experiments) are shown in the bar graph. Error bars represent the SEM. ***, $P < 0.0001$; ns, $P > 0.05$.

This finding is consistent with the similarity between this patient and the previously reported STIM1-deficient patients, who displayed severe opportunistic infection and autoimmunity (Picard et al., 2009). The other, previously reported STIM1-deficient patients displayed muscular hypotonia, partial iris hypoplasia, and dental enamel effects, which would probably not have been picked up in our patient because of the early onset and fatal outcome of KS.

We identified STIM1 deficiency as the first genetic etiology of isolated classic KS in childhood. The identification of STIM1 deficiency as the cause of severe KS in this child was based on the following evidence: (a) the patient presented autosomal recessive, complete STIM1 deficiency; (b) STIM1 deficiency has been reported to cause profound T cell deficiency in another sibship (Picard et al., 2009); (c) acquired T cell deficiencies are known risk factors for the development of KS; and (d) a genome-wide search for mutations in up to 95% of the genes present in the genome (based on National Center for Biotechnology Information Consensus Coding Sequence Database) failed to identify another plausible candidate mutation in the patient. We have excluded STIM1 deficiency in the other two Turkish children with KS who developed the disease later (at 9 yr of age), responded to treatment, and have remained well (Sahin et al., 2010; unpublished data). The whole-exome investigation of these patients would be expected to reveal other new genetic etiologies of KS, perhaps more specific to anti–HHV-8 immunity.

In recent months, whole-exome sequencing has led to identification of the molecular basis of rare Mendelian disorders in small numbers (two to four) of unrelated affected individuals (Hoischen et al., 2010; Lalonde et al., 2010; Ng et al., 2010), or in a single affected individual when used in conjunction with homozygosity mapping (Choi et al., 2009; Walsh et al., 2010). Our study provides the first evidence that whole-exome sequencing in a single patient can, without the aid of homozygosity mapping, lead to successful identification of the genetic basis of rare inborn errors, when combined with biochemical and cellular characterization to demonstrate the deleterious effect of the identified mutations. This approach may be particularly useful for deciphering new primary immunodeficiencies in children with sporadic, severe infections caused by a particular pathogen but without an overt immunological phenotype, not only rare phenotypes such as KS and herpes simplex encephalitis, but also more common infections, such as invasive pneumococcal disease and tuberculosis (Casanova and Abel, 2007; Alcaïs et al., 2009). Whole-exome sequencing in single patients with almost any sporadic phenotypes holds the promise to decipher both rare and common inborn errors.

MATERIALS AND METHODS

Massively parallel sequencing. 3 µg DNA extracted from EBV-B cells from the patient was sheared with Covaris S2 Ultrasonicator (Covaris). An adapter-ligated library was prepared with the Paired-End Sample Prep kit V1 (Illumina). Exome capture was performed with the SureSelect Human All Exon kit (Agilent Technologies). Single-end sequencing was performed on an Illumina Genome Analyzer IIx (Illumina), generating 72-base reads.

Sequence alignment, variant calling, and annotation. The sequences were aligned with the human genome reference sequence (hg18 build), using BWA aligner (Li and Durbin, 2009). Three open-source packages were used for downstream processing and variant calling: Genome analysis toolkit (GATK; McKenna et al., 2010), SAMtools (Li et al., 2009), and Picard Tools. Substitution calls were made with GATK UnifiedGenotyper, whereas indel calls were made with GATK IndelGenotyperV2. All calls with a read coverage ≤4x and a Phred-scaled SNP quality of ≤30 were filtered out. All the variants were annotated with SeattleSeq SNP annotation.

Genomic DNA sequencing. Genomic DNA was isolated from the EBV-B cells of the patient or the peripheral blood mononuclear cells of the family members. The 5′-CCTGGGAGAGTTGTAAAGCA-3′ and 5′-CCCAC-CACCAGGATATCTC-3′ primers were used to sequence *STIM1* exon 8 and its flanking intron regions.

Quantitative RT-PCR. Total RNA from EBV-B cells was used to generate cDNA with the SuperScript III First-Strand Synthesis System (Invitrogen). *STIM1* expression was assessed in the TaqMan gene expression assay (Hs00963373_m1; Applied Biosystems), with normalization of the results as a function of GUS (β-glucuronidase) gene expression.

Analysis of abnormally spliced *STIM1* transcripts. *STIM1* exons 7–9 were amplified from cDNA from the control or the patient's EBV-B cells, with the 5′-GGACTTGGAGGGGTTACAC-3′ and 5′-AGAGGATCTC-GATCTGTTGC-3′ primers. The amplicons were inserted into pCR2.1 with the TA cloning kit (Invitrogen) and sequenced with the same pair of primers. Sequences were analyzed with Lasergene software (DNASTAR).

Western blotting. Immunoblotting for STIM1 was performed with a monoclonal antibody against the N terminus of STIM1 (GOK; BD) or a rabbit polyclonal antibody against a 29-aa peptide at the C terminus of STIM1 (Picard et al., 2009). An antibody against GAPDH (Santa Cruz Biotechnology, Inc.) was used to demonstrate equal protein loading for each sample.

Retroviral transduction. Bicistronic plasmids encoding myc-tagged STIM1 or ORAI1, followed by IRES-GFP have been described elsewhere (Feske et al., 2006). EBV-B cells were transduced twice with VSV-G–pseudotyped retrovirus by spinoculation onto tissue culture plates coated with 10 μg/ml RetroNectin (TaKaRa). Transduction efficiency was assessed by evaluating the percentage of GFP^+ cells using flow cytometry.

Ca^{2+} flux measurement. Intracellular Ca^{2+} levels were measured by time-lapse single cell Ca^{2+} imaging, as previously described (Feske et al., 2005). In brief, EBV-B cells loaded with 1 μM Fura-2/AM (Invitrogen) were stimulated by passive store depletion with 1 μM thapsigargin (EMD Biosciences) in nominally Ca^{2+}-free Ringer's solution, followed by readdition of Ringer's solution containing 2 mM $CaCl_2$. Ca^{2+} levels were measured as the ratio of the emitted fluorescence at 340 and 380 nm (F340/F380) with an IX81 epifluorescence microscope (Olympus) and Slidebook imaging software v4.2 (Olympus). We analyzed >60 cells per experiment. For the analysis of intracellular Ca^{2+} levels in EBV-B cells transduced with retrovirus, we studied at least 48 GFP^+ and 48 GFP^- cells on average per experiment in 6–10 experiments per condition in total.

Online supplemental material. Table S1 provides the list of non-reported homozygous variations in the patient identified by whole-exome sequencing. Online supplemental material is available at http://www.jem.org/cgi/content/full/jem.20101597/DC1.

We thank the patient's family for their trust, and all members of the laboratory for helpful discussions.

The Laboratory of Human Genetics of Infectious Diseases is supported by grants from Institut National de la Santé et de la Recherche Médicale, University Paris Descartes, The Rockefeller University Center for Clinical and Translational Science grant number 5UL1RR024143-03, The Rockefeller University, and St. Giles Foundation. S. Feske is supported by National Institutes of Health grant AI066128. M. Byun is supported by Cancer Research Institute postdoctoral fellowship, and S. Plancoulaine is supported in part by a fellowship from Assistance Publique-Hôpitaux de Paris.

The authors have no conflicting financial interests. S. Feske is a co-founder of CalciMedica Inc. and a member of its scientific advisory board.

Submitted: 5 August 2010
Accepted: 14 September 2010

REFERENCES

Akman, E.S., U. Ertem, V. Tankal, A. Pamir, A.M. Tuncer, and O. Uluoglu. 1989. Aggressive Kaposi's sarcoma in children: a case report. *Turk. J. Pediatr.* 31:297–303.

Alcaïs, A., L. Abel, and J.L. Casanova. 2009. Human genetics of infectious diseases: between proof of principle and paradigm. *J. Clin. Invest.* 119:2506–2514. doi:10.1172/JCI38111

Bisceglia, M., M. Amini, and C. Bosman. 1988. Primary Kaposi's sarcoma of the lymph node in children. *Cancer.* 61:1715–1718. doi:10.1002/1097-0142(19880415)61:8<1715::AID-CNCR2820610833>3.0.CO;2-P

Boshoff, C., and R.A. Weiss. 2001. Epidemiology and pathogenesis of Kaposi's sarcoma-associated herpesvirus. *Philos. Trans. R. Soc. Lond. B Biol. Sci.* 356:517–534. doi:10.1098/rstb.2000.0778

Camcioglu, Y., C. Picard, V. Lacoste, S. Dupuis, N. Akçakaya, H. Cokura, G. Kaner, C. Demirkesen, S. Plancoulaine, J.F. Emile, et al. 2004. HHV-8-associated Kaposi sarcoma in a child with IFNgammaR1 deficiency. *J. Pediatr.* 144:519–523. doi:10.1016/j.jpeds.2003.11.012

Casanova, J.L., and L. Abel. 2007. Primary immunodeficiencies: a field in its infancy. *Science.* 317:617–619. doi:10.1126/science.1142963

Chang, Y., E. Cesarman, M.S. Pessin, F. Lee, J. Culpepper, D.M. Knowles, and P.S. Moore. 1994. Identification of herpesvirus-like DNA sequences in AIDS-associated Kaposi's sarcoma. *Science.* 266:1865–1869. doi:10.1126/science.7997879

Chang, Y., J. Ziegler, H. Wabinga, E. Katangole-Mbidde, C. Boshoff, T. Schulz, D. Whitby, D. Maddalena, H.W. Jaffe, R.A. Weiss, and P.S. Moore; Uganda Kaposi's Sarcoma Study Group. 1996. Kaposi's sarcoma-associated herpesvirus and Kaposi's sarcoma in Africa. *Arch. Intern. Med.* 156:202–204. doi:10.1001/archinte.156.2.202

Choi, M., U.I. Scholl, W. Ji, T. Liu, I.R. Tikhonova, P. Zumbo, A. Nayir, A. Bakkaloglu, S. Ozen, S. Sanjad, et al. 2009. Genetic diagnosis by whole exome capture and massively parallel DNA sequencing. *Proc. Natl. Acad. Sci. USA.* 106:19096–19101. doi:10.1073/pnas.0910672106

Dupin, N., M. Grandadam, V. Calvez, I. Gorin, J.T. Aubin, S. Havard, F. Lamy, M. Leibowitch, J.M. Huraux, J.P. Escande, et al. 1995. Herpesvirus-like DNA sequences in patients with Mediterranean Kaposi's sarcoma. *Lancet.* 345:761–762. doi:10.1016/S0140-6736(95)90642-8

Dutz, W., and A.P. Stout. 1960. Kaposi's sarcoma in infants and children. *Cancer.* 13:684–694. doi:10.1002/1097-0142(196007/08)13:4<684::AID-CNCR2820130408>3.0.CO;2-G

Erdem, T., M. Atasoy, N. Akdeniz, M. Parlak, and S. Ozdemir. 1999. A juvenile case of classic Kaposi's sarcoma. *Acta Derm. Venereol.* 79:492–493. doi:10.1080/000155599750010102

Ferrari, A., M. Casanova, G. Bisogno, G. Cecchetto, C. Meazza, L. Gandola, A. Garaventa, A. Mattke, J. Treuner, and M. Carli. 2002. Malignant vascular tumors in children and adolescents: a report from the Italian and German Soft Tissue Sarcoma Cooperative Group. *Med. Pediatr. Oncol.* 39:109–114. doi:10.1002/mpo.10078

Feske, S. 2009. ORAI1 and STIM1 deficiency in human and mice: roles of store-operated Ca2+ entry in the immune system and beyond. *Immunol. Rev.* 231:189–209. doi:10.1111/j.1600-065X.2009.00818.x

Feske, S., M. Prakriya, A. Rao, and R.S. Lewis. 2005. A severe defect in CRAC Ca2+ channel activation and altered K+ channel gating in T cells from immunodeficient patients. *J. Exp. Med.* 202:651–662. doi:10.1084/jem.20050687

Feske, S., Y. Gwack, M. Prakriya, S. Srikanth, S.H. Puppel, B. Tanasa, P.G. Hogan, R.S. Lewis, M. Daly, and A. Rao. 2006. A mutation in Orai1 causes immune deficiency by abrogating CRAC channel function. *Nature.* 441:179–185. doi:10.1038/nature04702

Ganem, D. 2010. KSHV and the pathogenesis of Kaposi sarcoma: listening to human biology and medicine. *J. Clin. Invest.* 120:939–949. doi:10.1172/JCI40567

Hoischen, A., B.W. van Bon, C. Gilissen, P. Arts, B. van Lier, M. Steehouwer, P. de Vries, R. de Reuver, N. Wieskamp, G. Mortier, et al. 2010. De novo mutations of SETBP1 cause Schinzel-Giedion syndrome. *Nat. Genet.* 42:483–485. doi:10.1038/ng.581

Hussein, M.R. 2008. Cutaneous and lymphadenopathic Kaposi's sarcoma: a case report and review of literature. *J. Cutan. Pathol.* 35:575–578. doi:10.1111/j.1600-0560.2007.00844.x

Kaposi, M. 1872. Idiopathisches multiples pigmentsarcom der haut. *Arch Dermatol und Syphillis.* 4:265–273. doi:10.1007/BF01830024

Lalonde, E., S. Albrecht, K.C. Ha, K. Jacob, N. Bolduc, C. Polychronakos, P. Dechelotte, J. Majewski, and N. Jabado. 2010. Unexpected allelic heterogeneity and spectrum of mutations in Fowler syndrome revealed by next-generation exome sequencing. *Hum. Mutat.* 31:918–923.

Landau, H.J., B.J. Poiesz, S. Dube, J.A. Bogart, L.B. Weiner, and A.K. Souid. 2001. Classic Kaposi's sarcoma associated with human herpesvirus 8 infection in a 13-year-old male: a case report. *Clin. Cancer Res.* 7:2263–2268.

Lebbé, C., C. Legendre, and C. Francès. 2008. Kaposi sarcoma in transplantation. *Transplant. Rev. (Orlando).* 22:252–261.

Li, H., and R. Durbin. 2009. Fast and accurate short read alignment with Burrows-Wheeler transform. *Bioinformatics*. 25:1754–1760. doi:10.1093/bioinformatics/btp324

Li, H., B. Handsaker, A. Wysoker, T. Fennell, J. Ruan, N. Homer, G. Marth, G. Abecasis, and R. Durbin; 1000 Genome Project Data Processing Subgroup. 2009. The Sequence Alignment/Map format and SAMtools. *Bioinformatics*. 25:2078–2079. doi:10.1093/bioinformatics/btp352

Martellotta, F., M. Berretta, E. Vaccher, O. Schioppa, E. Zanet, and U. Tirelli. 2009. AIDS-related Kaposi's sarcoma: state of the art and therapeutic strategies. *Curr. HIV Res.* 7:634–638. doi:10.2174/157016209789973619

McKenna, A.H., M. Hanna, E. Banks, A. Sivachenko, K. Cibulskis, A. Kernytsky, K. Garimella, D. Altshuler, S. Gabriel, M. Daly, and M. Depristo. 2010. The Genome Analysis Toolkit: A MapReduce framework for analyzing next-generation DNA sequencing data. *Genome Res.* 20:1297–1303.

Moore, P.S., and Y. Chang. 1995. Detection of herpesvirus-like DNA sequences in Kaposi's sarcoma in patients with and without HIV infection. *N. Engl. J. Med.* 332:1181–1185. doi:10.1056/NEJM199505043321801

Ng, S.B., K.J. Buckingham, C. Lee, A.W. Bigham, H.K. Tabor, K.M. Dent, C.D. Huff, P.T. Shannon, E.W. Jabs, D.A. Nickerson, et al. 2010. Exome sequencing identifies the cause of a mendelian disorder. *Nat. Genet.* 42:30–35. doi:10.1038/ng.499

Picard, C., F. Mellouli, R. Duprez, G. Chédeville, B. Neven, S. Fraitag, J. Delaunay, F. Le Deist, A. Fischer, S. Blanche, et al. 2006. Kaposi's sarcoma in a child with Wiskott-Aldrich syndrome. *Eur. J. Pediatr.* 165:453–457. doi:10.1007/s00431-006-0107-2

Picard, C., C.A. McCarl, A. Papolos, S. Khalil, K. Lüthy, C. Hivroz, F. LeDeist, F. Rieux-Laucat, G. Rechavi, A. Rao, et al. 2009. STIM1 mutation associated with a syndrome of immunodeficiency and autoimmunity. *N. Engl. J. Med.* 360:1971–1980. doi:10.1056/NEJMoa0900082

Sahin, G., A. Palanduz, G. Aydogan, O. Cassar, A.U. Ertem, L. Telhan, N. Canpolat, E. Jouanguy, C. Picard, A. Gessain, et al. 2010. Classic Kaposi sarcoma in 3 unrelated Turkish children born to consanguineous kindreds. *Pediatrics*. 125:e704–e708. doi:10.1542/peds.2009-2224

Schalling, M., M. Ekman, E.E. Kaaya, A. Linde, and P. Biberfeld. 1995. A role for a new herpes virus (KSHV) in different forms of Kaposi's sarcoma. *Nat. Med.* 1:707–708. doi:10.1038/nm0795-707

Walsh, T., H. Shahin, T. Elkan-Miller, M.K. Lee, A.M. Thornton, W. Roeb, A. Abu Rayyan, S. Loulus, K.B. Avraham, M.C. King, and M. Kanaan. 2010. Whole exome sequencing and homozygosity mapping identify mutation in the cell polarity protein GPSM2 as the cause of nonsyndromic hearing loss DFNB82. *Am. J. Hum. Genet.* 87:90–94. doi:10.1016/j.ajhg.2010.05.010

Zurrida, S., R. Agresti, and G. Cefalo. 1994. Juvenile classic Kaposi's sarcoma: a report of two cases, one with family history. *Pediatr. Hematol. Oncol.* 11:409–416. doi:10.3109/08880019409140540